

Characterization of Volatile Species Formed during Exposure of Photoresists to Ultraviolet Light

F. A. Houle,* V. R. Deline, H. Truong, and R. Sooriyakumaran

IBM Almaden Research Center, 650 Harry Road, San Jose, California 95120

Received April 2, 2007; Revised Manuscript Received July 26, 2007

ABSTRACT: A photochemical path for formation of volatile S and acidolytic paths for formation of volatile Si and/or C during exposure to ultraviolet light have been identified for two silicon-containing bilayer photoresists using atmospheric pressure ionization mass spectrometry (API MS) and secondary ion mass spectrometry (SIMS). Si and S are of particular concern because of their potential for irreversible adsorption onto nearby optical coatings inside a lithographic tool, causing permanent detuning. We describe the analytical techniques used and report estimates for absolute numbers of Si and S atoms lost from the resists. The data show that Si bound through oxygen is easily cleaved from the polymer by photogenerated acid while Si bound through carbon is not. Photodissociation of perfluorosulfonic acid from the photoacid generators results in significant loss of S. The data are compared to previous studies, and the advantages and limitations of these techniques for photoresist chemistry characterization are discussed.

Introduction

Polymer deprotection in the presence of photogenerated acid is the primary process of image formation in chemically amplified photoresists.¹ Deprotection is possible at all temperatures when acid is formed close to a protecting group and can be trapped by it without diffusion, but catalytic behavior leading to levels of deprotection suitable for changing polymer solubility² requires transport and hence elevated temperatures.³ When acidolytic deprotection occurs during exposure to UV light in a photolithography tool, vapors emitted from the exposed areas may chemisorb on adjacent lens surfaces.⁴ If the product flux is sufficient, a film can be formed that alters the lens' optical characteristics. Ever since the first reports of this problem⁵ there has been close scrutiny of all materials used inside the tools.⁶ This has been especially the case for very short wavelengths and resists such as silicon-containing bilayers since removal of silicon from optical coatings is much more difficult than removal of carbon.^{4,6–8}

Four primary methods have been used to screen for resist outgassing. The earliest technique reported was collection of emitted vapors in a cold trap with subsequent flash evaporation into a gas chromatograph–mass spectrometer (GC-MS) for analysis.^{5,9} This method collects all condensables and has the potential for uniquely identifying and quantifying all reaction products. It can miss any chemical classes that condense in the trap but do not re-evaporate, however. Also, reactions during the re-evaporation process can change the species detected by GC-MS, making it difficult to link a particular product to a specific primary chemical reaction or resist component. Typically GC-MS studies use a single column to separate various species in a mixture formed from all types of resists.⁵ This works well for certain cases; however, it has been shown that when this mixture contains, for example, hydrocarbons and siloxanes, multiple columns are required to cleanly separate all products.⁹

A second method is direct detection of products by mass spectrometry.^{8,10} In principle, this is an ideal technique since it removes the ambiguities of working with condensates, but it is rather insensitive so high laser energies and high resist

component concentrations can be required to produce sufficient signals. The ionization process involves electron-impact-induced fragmentation; therefore, the spectra obtained from a desorbing mixture can be difficult to assign. These measurements are typically done using a quadrupole mass spectrometer rather than a magnetic sector instrument, so sensitivities to various products are nonlinear with mass and gas product velocity and extensive calibrations are required for quantification.¹¹

The third method, usually complementing a GC-MS or direct MS measurement, is placement of a clean plate made of the same material as the lenses (usually called a proof plate) in front of a resist film during exposure to light and analysis of the material that condenses on it.^{4,7} This technique has the advantage of being both simple and the most relevant measurement since the outgassed products that are of greatest concern are those that can actually stick to a lens coating surface. It cannot be used to directly identify the specific outgassed chemicals that do condense, however, and requires very long exposure times to accumulate material detectable above normal background contaminant levels. Since the nucleation and growth process is nonlinear with time,¹² it is not possible to relate a measured amount of condensed products to an outgassing rate of a resist during exposure. Moreover, the use of accelerated deposition conditions⁷ may cause films to grow on optical surfaces that would not do so under normal exposure conditions.

Finally, an indirect method using API-MS¹³ for assessing available outgassing pathways by characterization of post-exposure bake (PEB) deprotection chemistry has been reported. Such measurements provide information on possible nonphotolytic outgassing pathways, with the assumption that acidolytic reactions at elevated temperature can also occur at room temperature, and are useful for screening the outgassing potential of materials containing heteroatoms such as silicon.^{14,15} While the API-MS method is extremely sensitive and is excellent for analyzing mixtures since no fragmentation occurs during ionization, it is blind to certain chemical species¹⁶ so can only present a partial picture of the reactions occurring. It requires authentic samples of all products at known partial pressures to be made fully quantitative, which is often not possible for polymer decomposition, although semiquantitative comparison

* Corresponding author. E-mail: houle@almaden.ibm.com.

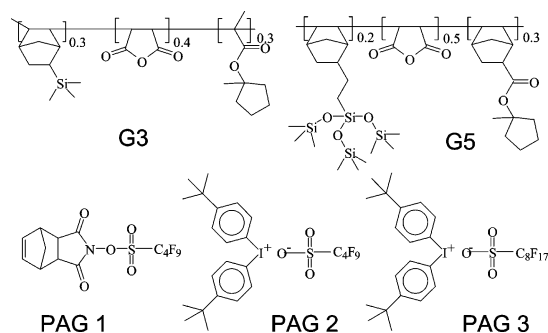


Figure 1. Structures of resist polymers and photoacid generators used in this work.

of analyte signals can be made. By probing only thermal pathways, photolytic formation of volatiles, likely to be increasingly important as wavelengths become shorter, are missed altogether.

It is clear that while each of these methods provides key information on aspects of the potential for lens contamination, each is difficult or impossible to make complete and quantitative. An assessment of the accuracy of an analysis is made even more difficult by the fact that the composition of commercial resists, which are of primary interest, is generally not disclosed. The major concern of the lithographic tool vendors is that the flux of outgassed species arriving at optical surfaces be held below that required for nucleation and growth of an unremovable condensate. The major concern of the resist designer is that offending outgassed molecules be identified in order to enable a redesign of the resist. In an effort to provide useful information that does not require extensive calibrations, we have developed a two-step analytical technique that combines the PEB studies using mass spectrometry described above with secondary ion mass spectrometry (SIMS) to determine elemental concentrations in a resist film before and after exposure. Purely thermal acidolytic reactions can be distinguished from photolytic reactions in favorable cases, and relative changes in elemental concentrations can be determined without prior knowledge of the resist composition. If the resist composition is known, the method is quantitative. We describe the measurements and apply them to outgassing of components from two 193 nm bilayer resist materials. As designed, these polymers contain silicon attached through passive pendant groups, that is, groups that do not serve as solubility switches and thus are not expected to react in the presence of photogenerated acid. It was expected that they should both show only outgassing of carbonaceous products bound through ester linkages. We have found, however, that this simple picture of the chemistry is not what is actually observed. In addition to providing a useful technique for quantification of outgassing, the measurements reported here provide new insight into the deprotection process in methacrylate-based lithographic resist polymers.

Experimental Section

Materials. Two resists, G3 and G5, were analyzed in this study. The polymer and photoacid generator (PAG) structures are shown in Figure 1. The acid-labile protecting group is methylcyclopentane in both cases, and the silicon-containing moieties are bound to norbornene.

The G3 synthesis has been reported elsewhere.¹⁷

Synthesis of 5-[Tris(trimethylsiloxy)silyl]ethyl-2-norbornene (G5 Monomer). Tris(trimethylsiloxy)silane (32.63 g, 0.11 mol) and 5-vinyl-2-norbornene (12 g, 0.10 mol) were placed in a round-bottom flask equipped with a magnetic stirrer, nitrogen inlet, and a water condenser. Platinum(0)–1,3-divinyl-1,1,3,3-tetramethylid-

Table 1. Elemental Concentrations (mol/cm²) in Resists

elements	G3	G5
C	5.801	5.090
O	1.347	1.675
S	1.88×10^{-2}	1.32×10^{-2}
Si	0.215	0.395
F	0.169	0.164

isiloxane complex in xylene (2.0 mL) was added to this mixture and heated at 70 °C for 19 h. Afterward, the mixture was distilled under reduced pressure to yield 35.20 g (78%) of the desired product at 130–132 °C at 2 mmHg pressure. ¹H NMR (ppm): 0.00–0.01 (27H, m), 0.33–0.41 (2H, m), 0.99–1.30 (5H, m), 1.73–1.85 (2H, m), 2.64–2.69 (2H, m), 5.80–6.02 (2H, m).

Synthesis of Terpolymer of 5-[Tris(trimethylsiloxy)silyl]ethyl-2-norbornene, 1-Methylcyclopentyl-5-norbornene-2-carboxylate, and Maleic Anhydride (G5 Polymer). 5-[Tris(trimethylsiloxy)silyl]ethyl-2-norbornene (4.17 g, 0.01 mol), 1-methylcyclopentyl-5-norbornene-2-carboxylate (3.40 g, 0.015 mol), maleic anhydride (2.45 g, 0.025 mol), and 10 g of ethyl acetate were placed in a round-bottom flask equipped with a condenser and a nitrogen inlet. 2,2'-Azobis(isobutyronitrile) (AIBN) (0.33 g, 0.002 mol) was added to this solution and stirred until dissolved. Then, the solution was degassed using four vacuum/nitrogen purges. The contents were then heated to reflux for 18 h. Afterward, the solution was added dropwise into methanol (500 mL). The precipitated polymer was filtered (frit), washed twice with methanol (50 mL), and dried under vacuum at 60 °C. Yield: 3.36 g; M_n = 4273; polydispersity: 1.40.

G3 contains PAGs 1 (6.5 wt %) and 2 (3.9 wt %), both from Aldrich. G5 contains PAGs 1 (5 wt %) and 3¹⁸ (3.5 wt %).

Film Preparation. Coated wafers were used for mass spectrometry of heated exposed and unexposed films, and neat resist polymer powders were used for thermogravimetric analysis with mass spectrometric detection. Wafers were prepared as a set (a single initial batch processed to post-apply bake (PAB) only, PAB + UV exposure (PE), and PAB + PE + post-expose bake (PEB)) to allow progressive composition changes to be tracked in a single measurement session. For all measurements the resist films were coated onto bare silicon wafers (no bottom antireflection coating) and post-apply baked at 130 °C for 60 s. They were exposed to 193 nm light in the reticle plane of an Ultratech ministepper to a dose of $4E_0$, 14.4 mJ/cm² for G3 and 32 mJ/cm² for G5. The post-expose bake step was performed at 130 °C for 60 s for the SIMS measurements and 10 min for the mass spectrometry measurements to ensure that all products had been swept through the inlet system.

Initial film thicknesses for SIMS samples were 209 nm for G3 and 302 nm for G5, the average of measurements at five separate locations using a Nanometrics Nanospec 6100. The film thicknesses were unchanged by exposure. The final thicknesses after PEB were 168 nm for G3 and 258 nm for G5. All SIMS wafers were cleaved immediately after preparation and specimens loaded into the vacuum chamber for pump-down overnight prior to analysis. The wafers used for mass spectrometry were of similar thickness (not measured) and were placed in the heated inlet system within 10 min after exposure. PAB-only films were studied within a day of preparation.

Using the initial film thicknesses, concentrations in mol/cm² for elements that were the targets of the SIMS measurements were calculated and are shown in Table 1.

Atmospheric Pressure Mass Spectrometry. The instrument and methods have been described in full elsewhere,^{13–15} with substitution of the Sciex TAGA mass spectrometer used previously with a Perkin-Elmer Biosystems Sciex API3+ mass spectrometer. Two types of measurements were made: analysis of vapors during thermolysis of neat polymer samples under nitrogen in a Perkin-Elmer TGS-2 thermogravimetric analyzer and analysis of vapors produced during post-expose bake in a heated, nitrogen-purged fast access cell. In both cases analyte is transported in a nitrogen flow to the source region of the mass spectrometer, ionized at atmospheric pressure by proton capture from ambient water ion clusters,

extracted into the mass spectrometer, and analyzed. Use of water clusters as ionization agents limits detection to species whose proton affinities are greater than that of water. Thus, while detection of most unsaturated and oxygen- and nitrogen-containing organics is facile, the instrument is blind to species such as benzene, alkanes, CO_2 , and SO_2 . The proton-transfer reaction does not cause fragmentation so each peak in the mass spectrum originates from a product species. A nitrogen gas curtain serves as a collision region at the entrance to the mass spectrometer to remove water molecules clustered to the analyte ions. This process is not completely efficient for all species, however, so occasionally both the analyte ions and their hydrates are detected.

Secondary Ion Mass Spectrometry. All measurements were made in negative secondary ion mode on a Cameca SC-Ultra SIMS instrument equipped with a Cs^+ source and a normal incidence electron flood gun. A 10–20 nm film of Pt was deposited on the surface of the photoresist films to provide a conductive reference plane for the secondary ion extraction optics. Nitrogen is a known contaminant in Pt deposition and results in an elevated CN^- signal just beneath the Pt film. The energy of the Cs^+ beam was 1 keV, and the current was 8.6 nA. The beam was rastered over an area of $200\text{ }\mu\text{m}$ by $200\text{ }\mu\text{m}$, and secondary ions were collected from a circular area $\sim 30\text{ }\mu\text{m}$ in diameter at the center of the raster. The charge neutralization was accomplished by having a reservoir of low-energy (near-thermal) electrons just above the sputtered surface that are available to compensate any positive charge buildup. The low-energy electrons cause much less damage to the photoresist than high-energy electrons which can also be used for charge neutralization. Even so, electron stimulated desorption of charge-labile elements such as F can and does occur, and the F^- signal is monitored to assess alignment of the electron and ion beams. This signal is small compared to the fluorine signal from sputtered resist. Typically, the repeatability of an implanted reference sample from a conductive matrix material such as silicon would be on the order of $\pm 1\%$ when normalized the matrix signal. The characterization of organic films is complicated by the charge neutralization process and its effect on the secondary ion optics;¹⁹ therefore, the repeatability has not been as good. In general, data obtained for a set of related samples within a few hours span are very repeatable, while comparison of absolute signal levels from day to day must be done cautiously. To be as self-consistent as possible, the SIMS data presented in this paper are from a single series measured over the course of a day. We repeated this measurement series numerous times over the course of several years as we learned to recognize artifacts, however, and we always observed the same trends in the data when the data are valid.

Sources of Error. The primary source of error in the SIMS analyses is incomplete charge neutralization and beam damage. When the measurement is well-controlled and stable, the absolute compositions are found to be reproducible to 2–5% depending on the element. We have found that instabilities can be sporadic, occurring at any time during a measurement. They are easily recognizable in the data and seem mainly to affect the scatter in signals from very stable negative ions such as F^- and CN^- from run to run on the same sample. Even when instabilities are present, the normalized element distributions for a given type of wafer (PAB, PE, PEB) are quite reproducible—only the absolute concentrations are affected. We are working on finding better ways to control analysis conditions so that scatter is minimized. Another primary source of error in the SIMS measurements is resist age. Degraded material, whose presence can be detected by lithographic performance characterization, leads to ion-bombardment-induced deprotection in exposed samples as revealed by erroneously high C and Si loss. Finally, because the SIMS measurements are performed in vacuum, it is possible that small molecules trapped in the resist are pumped away prior to measurement, leading to a larger apparent elemental loss than is actually occurring.

The major source of error in the mass spectrometry work stems from the technique itself—not all potential reaction products can be ionized by the source so the observed reaction paths are only a subset of what is actually occurring. Thus, it is important to not

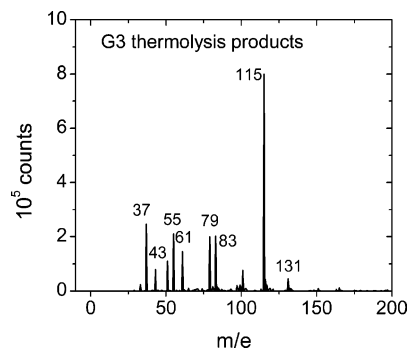


Figure 2. Thermogravimetric mass spectrometry data taken during thermolysis of G3 polymer in powder form at $\sim 200\text{ }^\circ\text{C}$ (background subtracted).

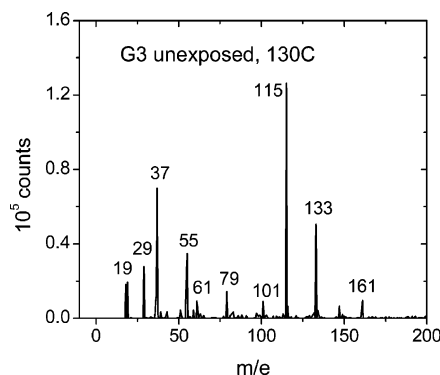


Figure 3. Mass spectrum of species desorbing from an unexposed cast film of G3 at $130\text{ }^\circ\text{C}$ after post-apply bake (background subtracted).

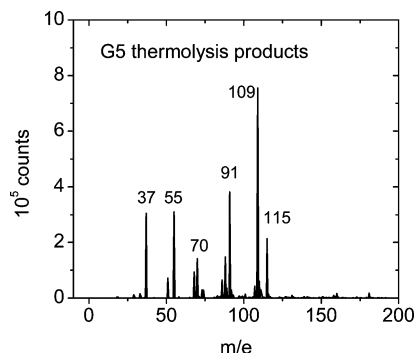


Figure 4. Thermogravimetric mass spectrometry data taken during thermolysis of G5 polymer in powder form at $\sim 230\text{ }^\circ\text{C}$ (background subtracted).

overinterpret the observations in terms of mechanisms. Reproducibility of relative peak intensities was excellent (within a few percent) over the course of this work.

Results and Discussion

Resist Polymer Decomposition at Elevated Temperature.

In order to be able to distinguish uniquely acidolytic and photochemical reactions, it is necessary to identify the primary nonacidolytic thermolysis decomposition pathways for G3 and G5 polymers. Using mass spectrometric detection, we have carried out both ramped temperature and isothermal studies. Thermogravimetric analyses of polymer powder decomposition were made over a range of $40\text{--}350\text{ }^\circ\text{C}$ using a heating ramp of $20\text{ }^\circ\text{C}/\text{min}$. Isothermal decompositions of films cast from propylene glycol monomethyl ether acetate (PGMEA) onto silicon wafers were carried out over a time of 5 min at $130\text{ }^\circ\text{C}$. Data are presented in Figures 2–5. Assignments for the most important peaks are given in Table 2. Amines, which are even numbered masses, appear to be present in the G5 sample. They

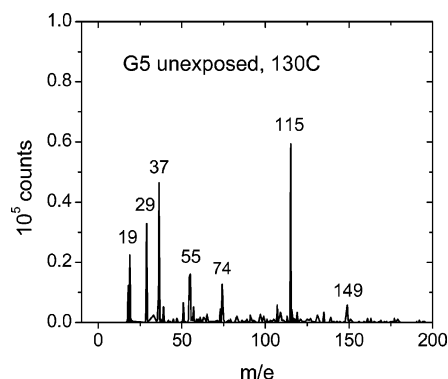


Figure 5. Mass spectrum of species desorbing from an unexposed cast film of G5 at 130 °C after post-apply bake (background subtracted).

Table 2. Mass Assignments for Major Peaks from G3 and G5 Polymer Thermolysis and Acidolysis^{a,b}

<i>m/e</i>	identity	G3	G5
43	propene·H ⁺	X	
61	propanol·H ⁺	X	
79	propanol·H ₃ O ⁺ ^c	X	
83	methylenecyclopentane·H ⁺	X	X
91	trimethylsilanol·H ⁺		X
109	trimethylsilanol·H ₃ O ⁺ ^c		X
115	C ₆ H ₁₁ O ₂ ⁺	X	X
163	hexamethyldisiloxane·H ⁺		X
181	hexamethyldisiloxane·H ₃ O ⁺ ^c		X

^a Alkanes, benzene, SO₂, and CO₂ cannot be detected using a hydronium ion source. ^b Mass peaks not listed: *m/e* 19, 37, 55, and 73 are protonated water clusters. *m/e* 133 is protonated PGMEA, the casting solvent. ^c Declustering in the ion source does not always remove all solvating waters from the ions, particularly from alcohols.

are likely to be at very low concentration, however, because the peaks are small despite the extremely high sensitivity of atmospheric pressure mass spectrometers to these compounds.¹⁶

A comparison of the thermolysis products from G3 and G5 show that both undergo cleavage at the ester to form methyl cyclopentyl radical, detected as methylene cyclopentane, but only G5 loses silicon-containing moieties. If there had been Si loss from G3, the expected product would have been dimethylsilylene (*m/e* 73) which we have observed in abundance in unpublished studies of polymers containing trimethylsilyl moieties attached through ester pendant groups. Because the method is blind to alkanes, detection of methylcyclopentane, the other methylcyclopentyl reaction product, is not possible.

Both polymers form significant peaks at *m/e* 115, whose identity has not been firmly established. Its empirical formula suggests that it is a pentenecarboxylic acid that could be formed by cleavage of the methylcyclopentene methacrylate group at the polymer backbone, with concurrent loss of methane. We have observed this decomposition pathway in other methacrylate polymers and copolymers. For example, typical thermolysis data are shown in Figure 6 for *p*-(*tert*-butyl methacrylate) (PTBMA). The primary peaks detected are *m/e* 57, protonated isobutylene, and *m/e* 87, whose formula is C₄H₇O₂⁺, assigned to protonated propene carboxylic acid. A search of the literature has led to a rather inconsistent description of how methacrylate polymers other than poly(methyl methacrylate) decompose since the original report appeared.²⁰ Complexities have been noted,²¹ and a direct investigation of poly(2-pentyl methacrylate) by GC with electron impact mass spectrometer detection has reported several unidentified products that have mass peaks that may be consistent with formation of a butenecarboxylic acid.²² Given the literature and the present observations, a reinvestigation of

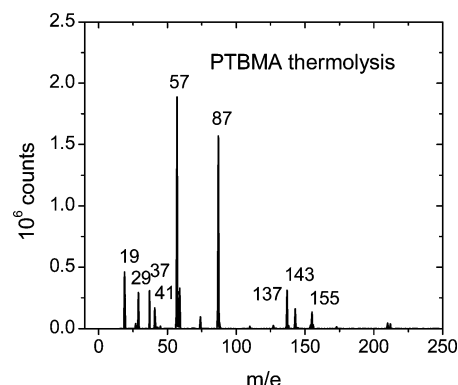


Figure 6. Thermogravimetric mass spectrometry data taken during thermolysis of PTBMA in powder form (background subtracted).

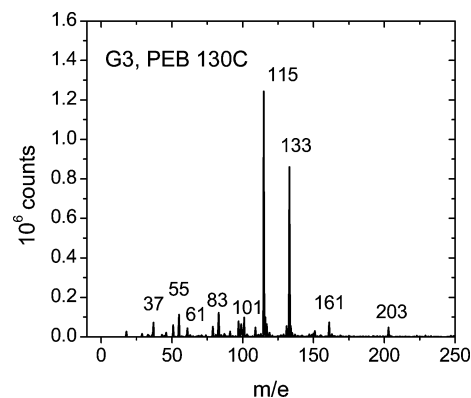


Figure 7. Mass spectrum of species desorbing during post-expose bake of a G3 resist film at 130 °C (background subtracted).

methacrylate polymer decomposition chemistry seems warranted.

A comparison of the mass spectra taken during polymer decomposition (around 200 °C) to those taken after heating at 130 °C for 5 min show that formation of the *m/e* 115 product is the lowest energy decomposition pathway detected. Loss of methylene cyclopentane and silanols prevail at higher temperatures. It is not possible from these data to infer relative quantities of alkenes and alcohols because the absolute mass spectral sensitivities to these compounds have not been determined. A limited study²³ of the relative sensitivity of alkenes, alcohols, and ketones/aldehydes has shown that the reactivity of characteristic moieties such as C=C and C=O double bonds and OH groups to water clusters tends to dominate sensitivity, with the order alkenes < alcohols << ketones, rather than the size of the R group involved. This is in agreement with a previous investigation that included a series of alcohols.¹⁶

Resist Acidolysis during Post-Exposure Bake. Typical mass spectra obtained during PEB of G3 and G5 at 130 °C are shown in Figures 7 and 8. It is noteworthy that for both the *m/e* 115 peak is intense, and much less methylene cyclopentane is formed than is observed thermally. The G5 spectra show significant new peaks at *m/e* 163 and 181, which are assigned to protonated hexamethyldisiloxane and hexamethyldisiloxane clustered to H₃O⁺. These data show that acid attacks at several locations on the G5 polymer: the ester pendant group with subsequent cleavage at the backbone and at the methylcyclopentane group and at siloxane (Si—O—Si—C) linkages. The C—Si—C bonds contained in G3 appear to be stable to acid attack. From these data we expect that any room temperature acidolysis that occurs during exposure will yield carbon-containing products from both G3 and G5, but silicon-containing products only from G5.

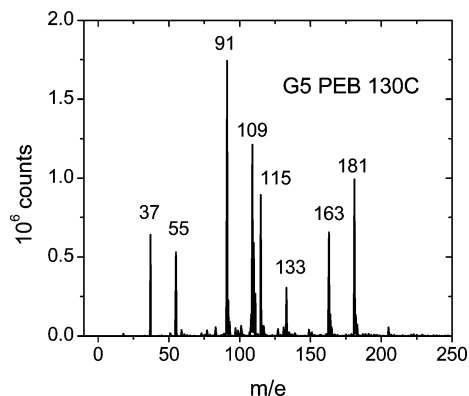


Figure 8. Mass spectrum of species desorbing during post-expose bake of a G5 resist film at 130 °C (background subtracted).

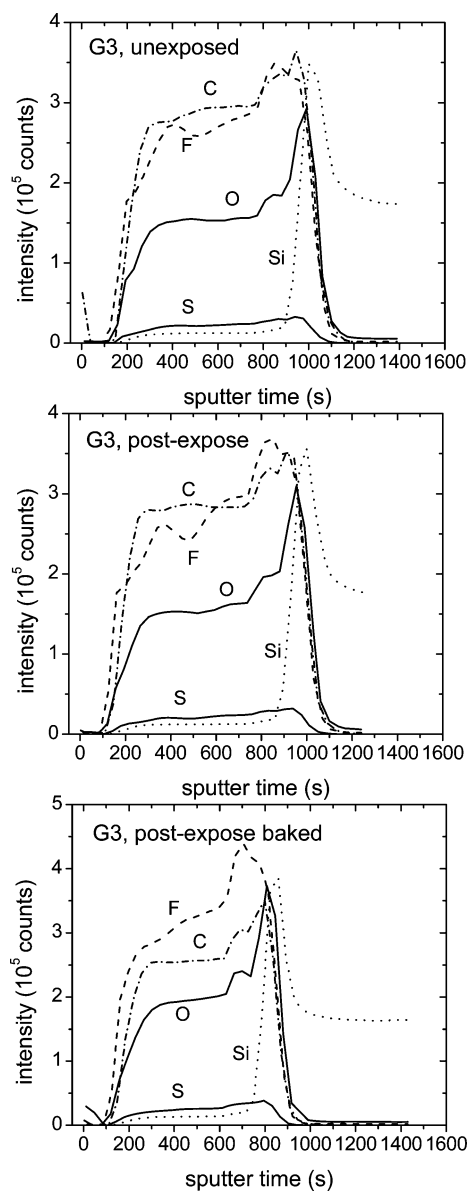


Figure 9. SIMS profiles for G3, unexposed, post-exposure, and post-expose baked. The film thicknesses are 209, 209, and 170 nm, respectively.

SIMS Measurements on Unexposed, Exposed, and Post-Expose Baked Resists. Depth profiles obtained for G3 and G5 unexposed, exposed, and post-expose baked films are shown in Figures 9 and 10. SIMS data are not quantitative without calibration because of differing ionization probabilities, which

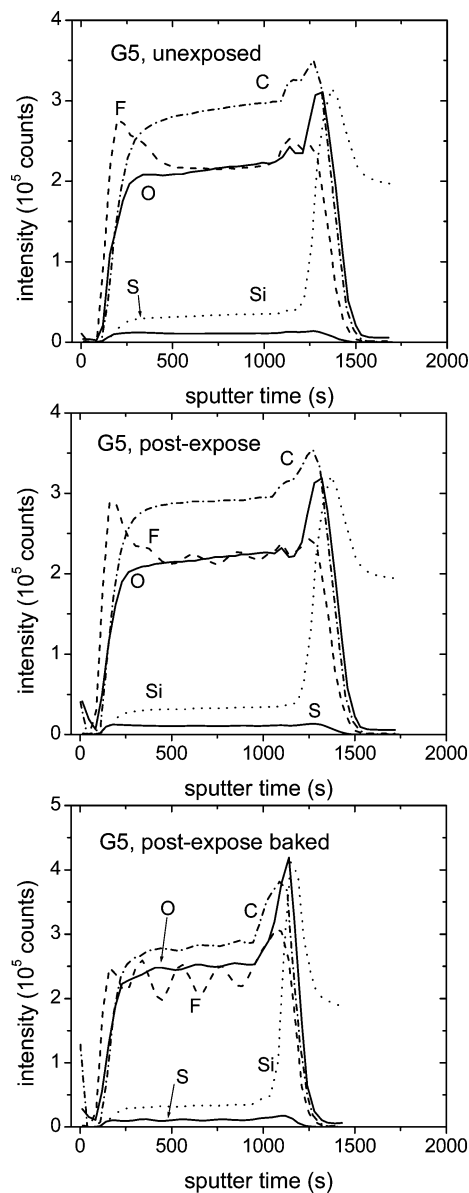


Figure 10. SIMS profiles for G5, unexposed, post-exposure, and post-expose baked. The film thicknesses are 302, 306, and 258 nm, respectively.

vary from element to element. Comparison of raw signals among closely related samples, such as the two series studied here, can be meaningful, however. Element concentrations were obtained by integrating the total ion signal as a function of depth through the film bulks, always using consistent criteria for setting the integration interval so that the integrated regions were a set fraction of the film thickness. Fluctuations at the top and bottom interfaces of the resist films are due to local composition and secondary ion extraction impacts on sensitivity, and therefore those data are not used in this analysis. It can be seen in Figure 9 that there are also fluctuations such as those in the F signals from the unexposed and post-expose film data for G3—these are typical of runs affected by sporadic instabilities in the measurements (probably from incomplete charge compensation) and serve to widen the error bars for the concentration determinations. The total signals for each data set were summed and relative concentration changes for each element obtained by normalizing signals to the totals. Two independent data sets were obtained for each sample and averaged to obtain the results presented in Table 3. The two sets were in agreement within 2%. The data show that after exposure the S concentration in

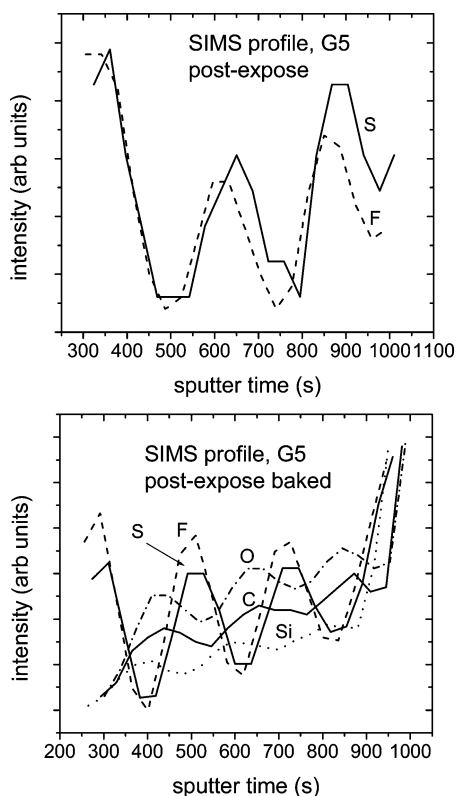


Figure 11. Periodic concentration variations as a function of depth in G5 films, resulting from standing waves in the resist during exposure. Exposed films show modulation in S and F from the photoacid generator. Post-expose baked films show additional anticorrelated modulation of C, O, and Si from the polymer.

the film decreases for both G3 and G5, while the Si concentration increases for G3 and decreases for G5. The change in S concentration was unexpected because at the time this work was done there had been no reports of S outgassing at 193 nm. A contemporaneous independent study on a different photoresist using direct mass spectrometry confirmed this result.²⁴

The data for G5 do not show the random fluctuations seen for G3. The post-expose data show clear periodic variations in the element signals that persist through post-expose bake. The data are plotted on an expanded scale in Figure 11. The presence of the variations is a result of standing waves in the films during illumination, a consequence of not using an antireflection layer under the resist. Three periods are detected, consistent with the incident wavelength (193 nm) and the thickness of the resist film (300 nm). Their presence in the S and F signals of the post-expose film establishes that PAG photolysis is a mechanism for the periodic concentration variations. Anticorrelated variations in C and O concentrations after PEB show that the photolyzed PAG concentration variations result in spatially varying extents of deprotection. It is not clear why they should be so pronounced in G5 but not G3—this is a result that has been reproduced many times during the course of this work. It may be that photoacid mobility is higher in G3 than in G5, perhaps because of a lack of trap sites, leading to a blurring of the standing waves.

The relative changes measured (Table 3) together with our knowledge of resist composition (Table 1) can be used to estimate absolute numbers of atoms lost during resist exposure. In SIMS it is not possible in general to compare raw signal intensities from one run to the next, thus requiring that an internal standard such as an elemental signal that is known to remain unchanged be used to normalize the data. Unfortunately

in exposed photoresists there is no completely unchanged elemental concentration. As an alternative we use the element with the highest concentration for this purpose, with the assumption that it loses the smallest number of atoms during exposure. This may not be a bad assumption: measurements show that the resist film thickness is unchanged by exposure, and the minor chemical changes that occur are unlikely to significantly alter the polymer density. We estimate the absolute values given in Table 4. Reasonable error limits for these values are difficult to set but are likely to be approximately a factor of 2. On exposure, the silicon concentration increases in G3 but decreases in G5, consistent with preferential loss of Si from the latter. From the mass spectrometry data this indicates that Si loss from G5 is due to acidolysis during and after exposure. The mechanism of acidolytic cleavage of Si-containing protecting groups bound through esters has been studied, explaining observations of siloxanes.²⁵ A GC-MS study of species outgassed from polymers using siloxane-containing protecting groups during exposure has shown Si loss in the range of $(1-2) \times 10^{14}$ Si/cm² (the resist thickness was not noted).⁹ What is interesting is that in the present case the Si is not attached through an ester but is nevertheless comparably labile. The lack of standing waves in the Si data for G3 and G5 show conclusively that there is no evidence for a photochemical route for Si-containing product formation, despite proposals in the literature that this may occur.⁸ The products detected by GC-MS are similar to those observed in the present work but differ from a separate GC-MS study identifying the primary outgassed species from an undisclosed polymer as $(\text{CH}_3)_3\text{SiF}$, formed by F abstraction by trimethylsilyl radical.⁸ This product was not detected in the present work, as expected since its negative ions are more stable than its positive ions,²⁶ but trimethylsilyl radical products such as dimethylsilylene were not either, indicating that there is no detectable route to its formation in the two polymers investigated in this work.

S, on the other hand, is clearly lost from both resists on exposure. The standing waves in the G5 depth profiles show that perfluorosulfonic acid photolysis is occurring. This is consistent with recent independent studies using electron impact mass spectrometry and 157⁸ and 193 nm²⁴ irradiation in which sulfur oxides were detected and proposed to originate from secondary photolysis of perfluorosulfonic acid. The present results indicate that for the PAGs used in this work S loss is of the order of 4% of the total PAG loading.

Our results are generally consistent with previous studies that have shown both PAG and deprotection products to be dominant among the species that desorb during resist exposure at 193 nm.^{6,8} Although quantitative values abound in the literature, comparison of those values to the data reported here is hampered by lack of complete information on resist thickness, light dose, and composition specifics such as identity of polymer and PAG concentration in the previous publications, in addition to some evolution in experimental protocols and accompanying assumptions.

There are some advantages and limitations to the addition of SIMS to available techniques for outgassing studies. The high sensitivity and large dynamic range of SIMS measurements allows resists to be formulated and exposed under normal conditions, not with high PAG loadings and high doses to improve signal levels. It is useful to be able to assess relative changes in elemental concentrations, which can be done with raw data, when the composition of a resist is not known. When the composition is known, quantitation is possible with a minimum of assumptions and no special requirements for calibrations. The problems with sporadic signal fluctuations do

Table 3. Elemental Signal Fractions Normalized to Total Signal for Each SIMS Profile

element	G3			G5		
	unexposed	exposed	PEB	unexposed	exposed	PEB
C	0.387	0.383	0.320	0.373	0.374	0.348
F	0.361	0.362	0.393	0.291	0.288	0.288
Si	0.0165	0.0167	0.0169	0.0426	0.0420	0.0409
S	0.0300	0.0288	0.0313	0.0144	0.0139	0.0140
O	0.206	0.209	0.238	0.280	0.282	0.309

Table 4. Estimated Changes in Numbers of Atoms per cm² of Resist

element	G3		G5	
	PE/unexp ^a	change in atoms ^b	PE/unexp ^a	change in atoms ^b
C	0.988	-8×10^{15}	0.999	-1×10^{15}
F	1	0	0.985	-4.3×10^{14}
Si	1.006	$+1.5 \times 10^{14}$	0.979	-1.4×10^{15}
S	0.958	-9×10^{13}	0.964	-8×10^{13}
O	1.012	$+2.6 \times 10^{15}$	1.002	$+4.3 \times 10^{14}$

^a Relative values calculated from Table 3. ^b Estimated absolute values.

limit the reliability of individual measurements, necessitating careful repeatability studies. We are also uncertain of the ultimate sensitivity achievable using this method, which depends on instrumental sensitivity to the elements of interest and on overcoming stability problems. The maximum permitted Si and S outgassing of a material depends on the limits set by lithographic tool vendors to avoid damage to optics. If this is much lower than about $1 \times 10^{13} \text{ cm}^{-2}$, improvements to the SIMS measurements will be required to extend the sensitivity to the required range.

Resist Deprotection. The data provide new insights to the deprotection pathways in these photoresist classes which are often poorly characterized because of the difficulties of working with systems at high concentration in the solid state. The observed acidolytic paths are cleavage of Si—O—Si—C linkages at sites other than the protected carboxylic acid, conventional deprotection, and cleavage at the polymer backbone. Photoresists are designed to have a certain concentration of ionizable OH groups after deprotection to optimize both sensitivity and dissolution. From the data presented here it should be recognized that after post-expose bake the polymer may be more chemically complex than previously appreciated. In particular, cleavage of the methacrylate ester at the polymer backbone will leave a significant density of permanently nonpolar groups that could result in random regions of marginally soluble material if the critical number of ionized groups cannot be reached.^{2,27} A more detailed investigation of this situation will allow a deeper understanding of the resist dissolution process and how it influences image imperfections such as line-edge roughness.

Conclusions

We have shown that SIMS can be used for a direct determination of elemental compositions changes during exposure due to outgassing. The method is applicable to resist films with normal PAG loadings and doses. The composition changes determined in this work, when coupled with mass spectrometry, show clear evidence for both photolytic and room temperature acidolytic deprotection sources for volatile species. The primary focus was on loss of species containing S and Si, which can form permanent deposits on optics in lithographic tools. Si loss occurs via room temperature acidolysis, and the SIMS and mass spectral data combined show that a Si—O—Si—C linkage in a pendant group is quite acid labile, while a C—Si—C group is

not. From the standing waves observed in G5 SIMS data and the very similar proportions of S lost from G3 and G5, we conclude that S loss is most likely to be photolytic. The lack of standing waves in the Si, C, and O SIMS data from exposed samples shows that direct or sensitized polymer decomposition does not occur to a significant extent. The observation that Si loss occurs in G5 by both mass spectrometry and SIMS but is not observed in G3 by either method suggests that mass spectrometric studies of post-expose bake chemistry can be used as a means for screening resist polymers for acidolytic reactions that are deleterious to exposure tools. Sulfonic acid photolysis to release S is apparently unavoidable. Although the SIMS analyses of these polymers required significant optimization, it was found to produce reliable and reproducible data when the correct experimental conditions were used. We believe that confidence limits of a factor of 2 are appropriate at this stage and are working toward improvement of our sensitivity and instrumental stability to lower our detection limits.

Acknowledgment. We are grateful to Rod Kunz (MIT Lincoln Laboratory) for his generous sharing of unpublished data and for many helpful discussions during the course of this work. We thank Dean Pearson (IBM) for his technical assistance with the API3+ and Robert Allen (IBM) for his interest and encouragement.

References and Notes

- Ito, H. *IBM J. Res. Dev.* **1997**, *41*, 69–80.
- Tsiartis, P. C.; Flanagan, L. W.; Henderson, C. L.; Hinsberg, W. D.; Sanchez, I. C.; Bonnacaze, R. T.; Willson, C. G. *Macromolecules* **1997**, *30*, 4656–4664.
- Hinsberg, W. D.; Houle, F. A.; Sanchez, M. I.; Wallraff, G. M. *IBM J. Res. Dev.* **2001**, *45*, 667–682.
- Kunz, R. R.; Liberman, V.; Downs, D. K. *J. Vac. Sci. Technol. B* **2000**, *18*, 1306–1313.
- Kunz, R. R.; Downs, D. K. *J. Vac. Sci. Technol. B* **1999**, *17*, 3330–3334.
- Meute, J.; Rich, G.; Hien, S.; Dean, K.; Gondran, C. *Proc. SPIE* **2002**, *4691*, 724–733.
- Hien, S.; Angood, S.; Ashworth, D.; Basset, S.; Bloomstein, T.; Dean, K.; Kunz, R. R.; Miller, D.; Patel, S.; Rich, G. *Proc. SPIE* **2001**, *4345*, 439–447.
- Kunz, R. R. *Proc. SPIE* **2004**, *5376*, 1–15.
- Barclay, G.; Kanagasabapathy, S.; Pohlers, G.; Mattia, J.; Xiong, K.; Ablaza, S.; Cameron, J.; Zampini, A.; Zhang, T.; Yamada, S.; Huby, F.; Wiley, K. *Proc. SPIE* **2003**, *5039*, 433–441.
- Watanabe, T.; Kinoshita, H.; Nii, H.; Hamamoto, K.; Tsubakino, H.; Hada, H.; Komano, H.; Irie, S. *J. Vac. Sci. Technol. B* **2001**, *19*, 736–742.
- Houle, F. A. *Int. J. Mass Spectrom. Ion Processes* **1993**, *123*, 243–252.
- Neugebauer, C. In *Handbook of Thin Film Technology*; Maissel, L. I., Glang, R., Eds.; McGraw-Hill: New York, 1970; Chapter 8.
- Prime, R. B.; Shushan, B. *Anal. Chem.* **1989**, *61*, 1195–1201.
- Houle, F. A.; Poliskie, G. M.; Hinsberg, W. D.; Pearson, D.; Sanchez, M. I.; Ito, H.; Hoffnagle, J. A. *Proc. SPIE* **2000**, *3999*, 181–187.
- Hinsberg, W. D.; Houle, F. A.; Poliskie, G. M.; Pearson, D.; Sanchez, M. I.; Ito, H. *J. Phys. Chem. A* **2002**, *106*, 9776–9787.
- Sunner, J.; Nicol, G.; Kebarle, P. *Anal. Chem.* **1988**, *60*, 1300–1307.
- Khojasteh, M. M.; Kwong, R. W.; Chen, K.-J.; Varanasi, P. K.; Allen, R. D.; Brock, P.; Houle, F.; Sooriyakumaran, R. US Patent 6,770,419, Aug 3, 2004.

- (18) Suzuki, Y.; Johnson, D. W. *Proc SPIE* **1998**, 3333, 735–746.
- (19) Deline, V. R. In *Materials and Process Characterization for VLSI 1988 (ICMPC'88)*; Zong, X.-F., Wang, Y.-Y., Chen, J., Eds.; World Scientific: Singapore, 1988; p 26.
- (20) Grant, D. H.; Grassie, N. *Polymer* **1960**, 1, 445–455.
- (21) Ito, H.; Ueda, M. *Macromolecules* **1988**, 21, 1475–1482.
- (22) Kojima, T.; Kurotu, T.; Masuda, K.-I.; Hosaka, Y. *J. Polym. Sci., Polym. Chem.* **1985**, 23, 343–349.
- (23) Houle, F. A., unpublished data.
- (24) Kunz, R. R., private communication, unpublished data.
- (25) Zharov, I.; Michl, J.; Sherwood, M.; Sooriyakumaran, R.; Larson, C. E.; DiPietro, R. A.; Breyta, G.; Wallraff, G. M. *Chem. Mater.* **2002**, 14, 656–663.
- (26) Lias, S. G.; Bartmess, J. E.; Liebman, J. F.; Holmes, J. L.; Levin, R. D.; Maillard, W. G. *J. Phys. Chem. Ref. Data* **1988**, 17 (Suppl. No. 1); www.webbook.nist.gov/chemistry, accessed March 19, 2007.
- (27) Houle, F. A.; Hinsberg, W. D.; Sanchez, M. I. *Macromolecules* **2002**, 35, 8591–8600.

MA070781P